

Proper orthogonal decomposition approach and error estimation of mixed finite element methods for the tropical Pacific Ocean reduced gravity model

Zhendong Luo^a, Jiang Zhu^b, Ruiwen Wang^b, I. M. Navon^{c*}

^a *School of Science, Beijing Jiaotong University, Beijing 100044, China*

^b *Institute of Atmospheric Physics, Chinese Academy of Sciences, Beijing 100029, China*

^c *Department of Mathematics and C.S.I.T., Florida State University, Dirac Sc. Lib. Bld., #470, Tallahassee, FL 32306–4120, USA*

Abstract

In this paper, the tropical Pacific Ocean reduced gravity model is studied using the proper orthogonal decomposition (POD) technique of mixed finite element (MFE) method, which is a model reduction technique for the simulation of physical processes governed by partial differential equations, e.g. fluid flows or other complex flow phenomena, and an error estimate of POD approximate solution based on MFE method is derived. It is shown by numerical examples that the error between POD approximate solution and reference solution is consistent with theoretical results, thus validating the feasibility and efficiency of POD method.

Keywords: Proper orthogonal decomposition technique; Mixed finite element method; Error estimate; Numerical simulation

1. Introduction

The variability of fluid flow and fluid total layer thickness over tropical oceans is an important question in studies of climate change and air–sea interaction. However, the accurate assessment of fluid flow and fluid total layer thickness is greatly limited due to the lack of direct measurements and the insufficient knowledge of air–sea exchange processes. The tropical Pacific Ocean reduced gravity model is a useful model to simulate fluid flow and fluid total layer thickness over tropical Pacific Ocean and it has been extensively applied to studying the ocean dynamics in tropical regions (see, Cane 1979[1]; Seager et al. 1988[2]). The model consists of two layers above the thermocline with the same constant density. The ocean below the thermocline, with a higher density, is assumed to be sufficiently deep so that its velocity vanishes (Figure 1). The upper of the two active layers is a fixed–depth surface layer in which the thermodynamics are included. The surface layer communicates with the lower active layer through entrainment/detrainment at their interface and through frictional horizontal shearing. We assume that there is no density difference across the base of the surface layer; that is, the surface layer is treated as part

*Corresponding author: Tel.: +1 850 644–6560; Fax: +1 850 644–0098.

E-mail address: navon@csit.fsu.edu (I. M. Navon)

of the upper layer.

Following Seager et al. (1988[2]), the equations for the depth—averaged currents are

$$\frac{\partial u}{\partial t} - fv = -g' \frac{\partial h}{\partial x} + \frac{\tau^x}{\rho_0 H} + A \nabla^2 u, \quad (1.1)$$

$$\frac{\partial v}{\partial t} + fu = -g' \frac{\partial h}{\partial y} + \frac{\tau^y}{\rho_0 H} + A \nabla^2 v, \quad (1.2)$$

$$\frac{\partial h}{\partial t} + H \left(\frac{\partial u}{\partial x} + \frac{\partial v}{\partial y} \right) = 0, \quad (1.3)$$

where (u, v) are the horizontal velocity components of the depth—averaged currents; h the total layer thickness; f the Coriolis force; H the mean depth of the layer; ρ_0 the density of water; g' Reduced gravity; and A the horizontal eddy viscosity coefficient, (τ^x, τ^y) the wind stress which is calculated by the aerodynamic bulk formula

$$(\tau^x, \tau^y) = \rho_a c_D |\mathbf{U}| (U, V),$$

where ρ_a is the density of the air; c_D the wind stress drag coefficient; $\mathbf{U} = (U, V)$ the wind speed vector; and (U, V) the components of the wind velocity. The seasonal net surface heat flux over tropical oceans has been only simulated with the equations (1.1)~(1.3) to add to a thermodynamics equation by Yu and O'Brien (see, [3]). However, since the computational field over the tropical Pacific ocean is too extensive, and nets is too most and is difficult to compute, fluid flow and fluid total layer thickness over tropical oceans is not simulated. Thus, an important problem is how to simplify the computational load and save time—consuming calculations and resource demands in the actual computational process in a sense that guarantees a sufficiently accurate numerical solution. Proper orthogonal decomposition (POD), also known as Karhunen—Loève expansions in signal analysis and pattern recognition (see [4]), or principal component analysis in statistics (see [5]), or the method of empirical orthogonal functions in geophysical fluid dynamics (see [6], [7]) or meteorology (see [8]), is a technique offering adequate approximate to represent fluid flow with reduced number of degrees of freedom, i.e., with lower dimensional models (see [9]) so as to simplify the computation and save CPU and memory requirements, and has found widespread applications in problems related to the approximation of large—scale models. Although the basic properties of POD method are well established and studies have been conducted to evaluate the suitability of this technique for various fluid flows (see [10], [11], and [12]), its applicability and limitations for actual fluid flow and fluid total layer thickness over the tropical Pacific Ocean are not well documented.

The POD method mainly provides a useful tool for efficiently approximating a large amount of data. The method essentially provides an orthogonal basis for representing the given data in a certain least squares optimal sense, that is, it provides a way to find optimal lower dimensional approximations of the given data. In addition to being optimal in a least squares sense, POD has

the property that it uses a modal decomposition that is completely data dependent and does not assume any prior knowledge of the process used to generate the data. This property is advantageous in situations where *a priori* knowledge of the underlying process is insufficient to warrant a certain choice of basis. Combined with the Galerkin projection procedure, POD provides a powerful method for generating lower dimensional models of dynamical systems that have a very large or even infinite dimensional phase space. The fact that this method always searches for linear (or affine) subspaces instead of curved submanifolds makes it computationally tractable. In many cases, the behavior of a dynamic system is governed by characteristics or related structures, even though the ensemble is formed by a large number of different instantaneous solutions. POD method can capture these temporal and spatial structures by applying a statistical analysis to the ensemble of data.

In fluid dynamics, Lumley first employed the POD technique to capture the large eddy coherent structures in a turbulent boundary layer (see [13]); this technique was further extended in [14], where a link between the turbulent structure and dynamics of a chaotic system was investigated. In Holmes et al [9], the overall properties of POD are reviewed and extended to widen the applicability of the method. The method of snapshots was introduced by Sirovich [15], and is widely used in applications to reduce the order of POD eigenvalue problem. Examples of these are optimal flow control problems [16~18] and turbulence [9, 13, 14, 19, 20].

In many applications of POD, the method is used to generate basis functions for a Reduced Order Model (ROM), which can simplify and provide quicker assessment of the major features of the fluid dynamics for the purpose of flow control demonstrated by Kurdila et al [18] or design optimization shown by Ly et al [17]. This application is used in a variety of other physical applications, such as in [17], which demonstrates an effective use of POD for a chemical vapor deposition (CVD) reactor.

In [21], though the tropical Pacific Ocean reduced gravity model is preliminarily dealt with POD method, an exact theoretical analysis was not carried out, in particular an error estimate of the POD approximate solution was not as yet derived. The objective of this paper is to investigate in depth to what extent can POD be successfully used to approximate the mixed finite element (MFE) solution for the tropical Pacific Ocean reduced gravity model. In particular we aim to provide an error estimate of the approximate MFE solution so that one could determine the number of required eigenmodes. Some numerical examples are provided for validating the proposed theory.

2. Outline of proper orthogonal decomposition technique

The essential problem of POD is to identify the underlying, coherent structures of a collected ensemble of data. This consists in finding the POD optimal bases and constructing a model of reduced dimension to approximate the original ensemble. Originally POD was used as a data representation technique. For model reduction of dynamical systems, POD may be used on data points derived from system trajectories obtained via experiments, numerical simulations, or analytical derivations.

2.1. Continuous case

Let $U_i(\bar{x}) (i = 1, 2, \dots, n)$ denote the set of n observations (also called snapshots) of some

physical process taken at position $\vec{x} = (x, y)$. The average of the ensemble of snapshots is given by

$$\bar{U} = \langle U \rangle = \frac{1}{n} \sum_{i=1}^n U_i(\vec{x}). \quad (2.1)$$

We form new ensemble by focusing on deviations from the mean as follows:

$$V_i = U_i - \bar{U}. \quad (2.2)$$

We wish to find an optimal compressed description of the sequence of data (2.2). One description of the process is a series expansion in terms of a set of basis functions. Intuitively, the basis functions should in some sense be representative of the members of the ensemble. Such a coordinate system, which possesses several optimality properties (to be discussed in the sequel), is provided by the Karhunen—Loève expansion (see [4]), where the basis functions Φ are, in fact, admixtures of the snapshots and are given by

$$\Phi = \sum_{i=1}^n a_i V_i(\vec{x}), \quad (2.3)$$

where the coefficients a_i are to be determined such that Φ given by (2.3) will most resemble the ensemble $\{V_i(\vec{x})\}_{i=1}^n$. More specifically, POD seeks a function Φ such that

$$\frac{1}{n} \sum_{i=1}^n |(V_i, \Phi)|^2 \quad (2.4)$$

subject to

$$(\Phi, \Phi) = \|\Phi\|^2 = 1 \quad (2.5)$$

is minimized, where (\cdot, \cdot) and $\|\cdot\|$ denote the usual L^2 —inner product and L^2 —norm, respectively.

It follows that (see, e.g., [22]) the basis functions are the eigenfunctions of the integral equation

$$\int_{\Omega} C(\vec{x}, \vec{x}') \Phi(\vec{x}') d\vec{x}' = \lambda \Phi(\vec{x}), \quad (2.6)$$

where the kernel is given by

$$C(\vec{x}, \vec{x}') = \frac{1}{n} \sum_{i=1}^n V_i(\vec{x}) V_i(\vec{x}'). \quad (2.7)$$

Substituting (2.3) into (2.6) yields the following eigenvalue problem:

$$\sum_{i=1}^n L_{i,j} a_j = \lambda a_i, \quad (2.8)$$

where $L_{ij} = \frac{1}{n}(V_i, V_j)$, $L = (L_{ij})_{n \times n}$ is a symmetric and nonnegative matrix. Thus we see that our problem amounts to solving for the eigenvectors of an $n \times n$ matrix where n is the size of the ensemble of snapshots. Straightforward calculation (see also [22]) shows that the cost functional

$$\frac{1}{n} \sum_{i=1}^n |(V_i, \Phi)|^2 = (\lambda \Phi, \Phi) = \lambda,$$

is maximized when the coefficients a_i ($i=1, 2, \dots, n$) of (2.8) are the elements of the eigenvector corresponding to the largest eigenvalue of L .

2.2. Discrete case

Alternatively, we also can consider the discrete Karhunen—Loève expansion to find an optimal representation of the ensemble of snapshots. In general, each sample of snapshots $U_i(\bar{x})$ (defined on a set of m nodal points \bar{x}) can be expressed as a m dimensional vector \vec{u}_i as follows:

$$\vec{u}_i = [u_{i1}, u_{i2}, \dots, u_{im}]^T, \quad (2.9)$$

where u_{ij} denotes the j -th component of the vector \vec{u}_i . The mean vector is given by

$$\bar{u}_k = \frac{1}{n} \sum_{i=1}^n u_{ik}, k = 1, \dots, m. \quad (2.10)$$

We also can form a new ensemble by focusing on deviations from the mean value as follows

$$v_{ik} = u_{ik} - \bar{u}_k, k = 1, \dots, m. \quad (2.11)$$

Let the matrix A denotes the new ensemble

$$A = \begin{pmatrix} v_{11} & v_{21} & \cdots & v_{n1} \\ v_{12} & v_{22} & \cdots & v_{n2} \\ \vdots & \vdots & \vdots & \vdots \\ v_{1m} & v_{2m} & \cdots & v_{nm} \end{pmatrix}_{m \times n},$$

where the discrete covariance matrix of the ensemble \vec{u} may be written as

$$C y_k = A A^T y_k = \lambda_k y_k. \quad (2.12)$$

Thus, to compute the POD mode, one must solve a $m \times m$ eigenvalue problem. For a discretization of an ocean problem, the dimension m often exceeds 10^4 , so that a direct solution of this eigenvalue problem is often not feasible. We can transform the $m \times m$

eigenvalue problem into an $n \times n$ eigenvalue problem (see [23]). In the method of snapshots, one then solves the $n \times n$ eigenvalue problem

$$Dw_k = A^T Aw_k = \lambda_k w_k, \quad w_k \in R^n, \quad (2.13)$$

where the eigenvalues $\lambda_k (1 \leq k \leq n)$ are the same in (2.8). The eigenvectors w_k may be chosen to be orthonormal, and the POD modes are given by $\phi_k = Aw_k / \sqrt{\lambda_k}$. In matrix form, with $\Phi = [\phi_1, \dots, \phi_n]$, and $W = [w_1, \dots, w_n]$, this becomes $\Phi = AW$.

The $n \times n$ eigenvalue problem (2.13) is more efficient than the $m \times m$ eigenvalue problem (2.12) when the number of snapshots n is much smaller than the number of states m .

3. POD technique and error estimate of MFE method for tropical Pacific Ocean reduced gravity model

In this section, we apply the POD technique and MFE method to the upper tropical Pacific Ocean model described in Section 1. This method provides a systematic way of creating a reduced basis space using the state of the system at n different time instances. As in the general reduced order basis methods, the states could come from full order numerical computations (also obtained from system trajectories obtained via experiments, or analytical derivations). Here, we apply the MFE methods to the upper tropical Pacific ocean model for obtaining full order numerical solution, then apply the POD technique to reconstruct the approximate solution and approximate the solution of the reduced model. Finally, we compare the error of the accurate solution with that of the approximate solution.

3.1. MFE method for the tropical Pacific Ocean reduced gravity model

The Sobolev spaces along with their properties used in this context are standard (cf. Ref. [24]). Let $L_0^2(\Omega) = \left\{ q \in L^2(\Omega); \int_{\Omega} q dx = 0 \right\}$. For the sake of convenience, we consider the mixed variational formulation for (1.1) ~ (1.3) with the boundary conditions

$$u(x, y, t)|_{\partial\Omega} = 0, v(x, y, t)|_{\partial\Omega} = 0, h(x, y, t)|_{\partial\Omega} = 0, 0 \leq t \leq t_1,$$

and initial condition

$$u(x, y, 0) = u^0(x, y), \quad v(x, y, 0) = v^0(x, y), \quad h(x, y, 0) = h^0(x, y), \quad (x, y) \in \Omega.$$

Problem (I). Find $(u, v, h) \in H_0^1(\Omega) \times H_0^1(\Omega) \times L_0^2(\Omega)$ such that

$$\begin{cases} (u_t, \varphi) - f(v, \varphi) - g'(h, \varphi_x) + A(\nabla u, \nabla \varphi) = (f_1, \varphi), & \forall \varphi \in H_0^1(\Omega), \\ (v_t, \psi) + f(u, \psi) - g'(h, \psi_y) + A(\nabla v, \nabla \psi) = (f_2, \psi), & \forall \psi \in H_0^1(\Omega), \\ (h_t, q) + H(u_x + v_y, q) = 0, & \forall q \in L_0^2(\Omega), \end{cases}$$

where $f_1 = \frac{\tau^x}{\rho_0 H}$, $f_2 = \frac{\tau^y}{\rho_0 H}$. Using the same as approach in ref. [25], we could check that

Problem (I) has a unique solution.

In order to find the numerical solution for Problem (I), it is necessary to discretize Problem (I). We introduce a finite element approximation for spatial variable and finite difference scheme for the time derivative. Let \mathfrak{T}_h be a uniform regular triangulation of $\overline{\Omega}$ (here Ω denotes the two dimensional rectangular domain as depicted in Figure 1, is chosen from 30° S to 30° N in latitude and from 130° E to 70° W in longitude in actual computation), i.e., for any $K \in \mathfrak{T}_h$, put $h_K = \text{diam}\{K\}$, $h = \max_{K \in \mathfrak{T}_h} \{h_K\}$, then $c\bar{h} \leq h \leq c_1\bar{h}$. Denote the time step increment by $k = T_1/n$ (T_1 being the total time) and MFE approximation of (u, v, h) by $(u_h^i, v_h^i, h_h^i) = (u_h(t_i), v_h(t_i), h_h(t_i))$, $t_i = ik$ ($0 \leq i \leq n$). Define the finite element subspaces $H_0^1(\Omega)$ and $L_0^2(\Omega)$ as follows, respectively,

$$\begin{cases} X_h = \{\varphi_h \in H_0^1(\Omega); \varphi_h|_K \in P_m(K), \forall K \in \mathfrak{T}_h\}, \\ L_h = \{q_h \in L_0^2(\Omega); q_h|_K \in P_{m-1}(K), \forall K \in \mathfrak{T}_h\}, \end{cases}$$

where $m \geq 1$ is integer, $P_m(K)$ polynomial subspace of degrees $\leq m$ on K . Then, the fully discrete formulation for Problem (I) can be written as:

Problem (II). Find $(u_h^i, v_h^i, h_h^i) \in X_h \times X_h \times L_h$ ($i = 1, 2, \dots, n$) such that

$$\begin{cases} (u_h^i, \varphi_h) - kf(v_h^i, \varphi_h) - kg'(h_h^i, \varphi_{hx}) + kA(\nabla u_h^i, \nabla \varphi_h) = k(f_1^i, \varphi_h) + (u_h^{i-1}, \varphi_h), \\ \quad \forall \varphi_h \in X_h, \\ (v_h^i, \psi_h) + kf(u_h^i, \psi_h) - kg'(h_h^i, \psi_{hy}) + kA(\nabla v_h^i, \nabla \psi_h) = k(f_2^i, \psi_h) + (v_h^{i-1}, \psi_h), \\ \quad \forall \psi_h \in X_h, \\ (h_h^i, q_h) + kH(u_{hx}^i + v_{hy}^i, q_h) = (h_h^{i-1}, q_h), \quad \forall q_h \in L_h, \quad i = 1, 2, \dots, n, \\ u_h^0 = u^0(x, y), v_h^0 = v^0(x, y), h_h^0 = h^0(x, y), \end{cases}$$

where $f_1^i = f_1(t_i)$, $f_2^i = f_2(t_i)$. Using the same as approach as in [26], we could check that

Problem (II) has unique solution $(u_h^i, v_h^i, h_h^i) \in X_h \times X_h \times L_h$, and if solution $(u, v, h) \in H^{m+1}(\Omega) \times H^{m+1}(\Omega) \times H^m(\Omega)$ of Problem (I), the following error estimates hold

$$\left\{ \begin{array}{l} \|u(t_i) - u_h^i\|_0 + k^{1/2} \sum_{j=1}^i \|\nabla(u(t_j) - u_h^j)\|_0 \leq c(\tilde{h}^m + k), \\ \|v(t_i) - v_h^i\|_0 + k^{1/2} \sum_{j=1}^i \|\nabla(v(t_j) - v_h^j)\|_0 \leq c(\tilde{h}^m + k), \\ \|h(t_i) - h_h^i\|_0 \leq c(\tilde{h}^m + k), \quad i = 1, 2, \dots, n, \end{array} \right. \quad (3.1)$$

where c is a constant independent of \tilde{h} and k , but dependent of (u, v, h) .

3.2. POD technique for the tropical Pacific Ocean reduced gravity model

In the construction described above Section 2, the number n may be large, depending on the complexity of the dynamics represented in the ‘‘snapshots’’ $U_i(x, y) = (u_h^i, v_h^i, h_h^i)$ ($1 \leq i \leq n$).

In general, one should take n sufficiently large so that the snapshots $U_i(x, y)$ contain all salient features of the dynamics being investigated. Thus, the POD basis functions Φ_i ($1 \leq i \leq n$), used with the original dynamics in a Galerkin procedure, offer the possibilities of achieving a high fidelity model albeit with perhaps a large dimension n .

To apply the POD techniques to the upper tropical Pacific ocean model in Section 1, we first solve Problem (II) at n (for example, $n=30$) time steps and obtain the snapshots for the solutions of upper layer thickness and velocity field in the following (u_h^i, v_h^i, h_h^i) ($i = 1, 2, \dots, n$)

at an increment of T_1/n (for example, $T_1 = 1$ year) day for $(x, y) \in \Omega$. These snapshots are discrete data over Ω . Using (2.10), (2.11), and (2.13) yields covariance matrix $D_h = A_h^T A_h$,

$D_u = A_u^T A_u, D_v = A_v^T A_v$ associated with (u_h^i, v_h^i, h_h^i) ($i = 1, 2, \dots, n$). Since D_h, D_u, D_v are all nonnegative Hermitian matrices, they all have a complete set of orthogonal eigenvectors with the corresponding eigenvalues arranged in ascending order as $\lambda_1^h \geq \lambda_2^h \geq \dots \geq \lambda_n^h \geq 0$;

$\lambda_1^u \geq \lambda_2^u \geq \dots \geq \lambda_n^u \geq 0; \lambda_1^v \geq \lambda_2^v \geq \dots \geq \lambda_n^v \geq 0$, respectively. Then we construct POD basis

elements $\Phi_i^h(x, y), \Phi_i^u(x, y), \Phi_i^v(x, y)$ such that

$$\left\{ \begin{array}{l} X_u^{POD} = \mathbf{span}\{\Phi_1^u(x, y), \Phi_2^u(x, y), \dots, \Phi_n^u(x, y)\}, \\ X_v^{POD} = \mathbf{span}\{\Phi_1^v(x, y), \Phi_2^v(x, y), \dots, \Phi_n^v(x, y)\}, \\ X_h^{POD} = \mathbf{span}\{\Phi_1^h(x, y), \Phi_2^h(x, y), \dots, \Phi_n^h(x, y)\} \end{array} \right. \quad (3.2)$$

are defined as

$$\Phi_j^u = \sum_{i=1}^n a_{ui}^j u_h^i; \quad \Phi_j^v = \sum_{i=1}^n a_{vi}^j v_h^i; \quad \Phi_j^h = \sum_{i=1}^n a_{hi}^j c_h^i, \quad (3.3)$$

Where $a_{hi}^j, a_{ui}^j, a_{vi}^j$ ($1 \leq i \leq n$) are the components of the eigenvectors $A_h V_h^j / \sqrt{\lambda_{hj}}$, $A_u V_u^j / \sqrt{\lambda_{uj}}$, $A_v V_v^j / \sqrt{\lambda_{vj}}$ corresponding to the eigenvalues $\lambda_j^u, \lambda_j^v, \lambda_j^h$ ($1 \leq j \leq n$), respectively.

Since $\Phi_i^h(\vec{x}); \Phi_i^u(\vec{x}); \Phi_i^v(\vec{x})$ ($i = 1, 2, \dots, n$) are three groups of basic functions, the solution of Problem (II) could be uniquely written as

$$\begin{cases} u_h^s = \bar{u}(x, y) + \sum_{j=1}^n \beta_j^u(t_s) \Phi_j^u(x, y), \\ v_h^s = \bar{v}(x, y) + \sum_{j=1}^n \beta_j^v(t_s) \Phi_j^v(x, y), \quad 1 \leq s \leq n, \\ h_h^s = \bar{h}(x, y) + \sum_{j=1}^n \beta_j^h(t_s) \Phi_j^h(x, y), \end{cases} \quad (3.4)$$

where β_i^u ($i = 1, \dots, n$), β_i^v ($i = 1, \dots, n$), and β_i^h ($i = 1, \dots, n$) are uniquely determined coefficients; $\bar{u}(x, y)$, $\bar{v}(x, y)$, and $\bar{w}(x, y)$ are the mean values of (u_h^i, v_h^i, h_h^i) ($i = 1, 2, \dots, n$), respectively. Since the scales in model variables u, v and h are not uniform, one may employ different modes to reconstruct the solutions. In order to reduce order for Problem (II), we apply the POD approximate solution

$$\begin{cases} u_{M_1}^s = \bar{u}(x, y) + \sum_{i=1}^{M_1} \beta_i^u(t_s) \Phi_i^u(x, y), \\ v_{M_1}^s = \bar{v}(x, y) + \sum_{j=1}^{M_1} \beta_j^v(t_s) \Phi_j^v(x, y), \quad 1 \leq s \leq n, \\ h_{M_2}^s = \bar{h}(x, y) + \sum_{l=1}^{M_2} \beta_l^h(t_s) \Phi_l^h(x, y), \end{cases} \quad (3.5)$$

where β_i^u ($i = 1, \dots, M_1$), β_j^v ($j = 1, \dots, M_1$), β_l^h ($l = 1, \dots, M_2$), $\bar{u}(x, y)$, $\bar{v}(x, y)$, and $\bar{w}(x, y)$ are the same as equations (3.6). Substituting the solutions (u_h^n, v_h^n, h_h^n) of Problem (II) with (3.4) and (3.5), respectively, we could obtain the following equations, respectively.

Problem (III). Find $(\beta_r^u(t_s), \beta_r^v(t_s), \beta_r^h(t_s))$ ($r = 1, 2, \dots, n$) such that

$$\left\{ \begin{array}{l} \beta_r^u(t_s) - kf \sum_{j=1}^n \beta_j^v(t_s)(\Phi_j^v, \Phi_r^u) - kg' \sum_{l=1}^n \beta_l^h(t_s)(\Phi_l^h, \Phi_{rx}^u) + kA \sum_{i=1}^n \beta_i^u(t_s)(\nabla \Phi_i^u, \nabla \Phi_r^u) \\ \quad = k(f_1^s, \Phi_r^u) + \beta_r^u(t_{s-1}), \\ \beta_r^v(t_s) + kf \sum_{i=1}^n \beta_i^u(t_s)(\Phi_j^u, \Phi_r^v) - kg' \sum_{l=1}^n \beta_l^h(t_s)(\Phi_l^h, \Phi_{ry}^v) + kA \sum_{j=1}^n \beta_j^v(t_s)(\nabla \Phi_j^v, \nabla \Phi_r^v) \\ \quad = k(f_2^s, \Phi_r^v) + \beta_r^v(t_{s-1}), \\ \beta_r^h(t_s) + kH \sum_{i=1}^n \beta_i^u(t_s)(\Phi_i^u, \Phi_{rx}^h) + kH \sum_{j=1}^n \beta_j^v(t_s)(\Phi_j^v, \Phi_{ry}^h) = \beta_r^h(t_{s-1}), \\ \quad r = 1, 2, \dots, n, \quad s = 1, 2, \dots, n, \end{array} \right.$$

along with the initial condition

$$\left\{ \begin{array}{l} \beta_i^u(0) = (u(x, y, 0) - \bar{u}(x, y), \Phi_i^u(x, y)), \\ \beta_i^v(0) = (v(x, y, 0) - \bar{v}(x, y), \Phi_i^v(x, y)), \quad 1 \leq i \leq n. \\ \beta_i^h(0) = (v(x, y, 0) - \bar{v}(x, y), \Phi_i^h(x, y)), \end{array} \right. \quad (3.7)$$

Problem (IV). Find $(\beta_r^u(t_s), \beta_r^v(t_s), \beta_\ell^h(t_s))$ ($r = 1, 2, \dots, M_1, \ell = 1, 2, \dots, M_2$) such that

$$\left\{ \begin{array}{l} \beta_r^u(t_s) - kf \sum_{j=1}^{M_1} \beta_j^v(t_s)(\Phi_j^v, \Phi_r^u) - kg' \sum_{l=1}^{M_2} \beta_l^h(t_s)(\Phi_l^h, \Phi_{rx}^u) + kA \sum_{i=1}^{M_1} \beta_i^u(t_s)(\nabla \Phi_i^u, \nabla \Phi_r^u) \\ \quad = k(f_1^s, \Phi_r^u) + \beta_r^u(t_{s-1}), \quad r = 1, 2, \dots, M_1, \\ \beta_r^v(t_s) + kf \sum_{i=1}^{M_1} \beta_i^u(t_s)(\Phi_j^u, \Phi_r^v) - kg' \sum_{l=1}^{M_2} \beta_l^h(t_s)(\Phi_l^h, \Phi_{ry}^v) + kA \sum_{j=1}^{M_1} \beta_j^v(t_s)(\nabla \Phi_j^v, \nabla \Phi_r^v) \\ \quad = k(f_2^s, \Phi_r^v) + \beta_r^v(t_{s-1}), \quad r = 1, 2, \dots, M_1, \\ \beta_\ell^h(t_s) + kH \sum_{i=1}^{M_1} \beta_i^u(t_s)(\Phi_i^u, \Phi_{\ell x}^h) + kH \sum_{j=1}^{M_1} \beta_j^v(t_s)(\Phi_j^v, \Phi_{\ell y}^h) = \beta_\ell^h(t_{s-1}), \\ \quad \ell = 1, 2, \dots, M_2, \quad s = 1, 2, \dots, n, \end{array} \right.$$

along with the initial condition

$$\left\{ \begin{array}{l} \beta_i^u(0) = (u(x, y, 0) - \bar{u}(x, y), \Phi_i^u(x, y)), \quad 1 \leq i \leq M_1; \\ \beta_i^v(0) = (v(x, y, 0) - \bar{v}(x, y), \Phi_i^v(x, y)), \quad 1 \leq i \leq M_1; \\ \beta_\ell^h(0) = (v(x, y, 0) - \bar{v}(x, y), \Phi_\ell^h(x, y)), \quad 1 \leq \ell \leq M_2. \end{array} \right. \quad (3.8)$$

Solving the above Problem (IV) we can obtain the reconstructed solutions for the reduced model of Problem (III).

3.3. Error estimate of POD approximate solutions for tropical Pacific Ocean reduced gravity model

In the following, we derive the error estimate between the solutions for Problem (III) and the solutions for Problem (IV). To this end, subtracting Problem (IV) and (3.8) from Problem (III) and (3.7) yields the following error equations.

$$\left\{ \begin{array}{l}
\beta_r^u(t_s) - kf \sum_{j=M_1+1}^n \beta_j^v(t_s)(\Phi_j^v, \Phi_r^u) - kg' \sum_{l=M_2+1}^n \beta_l^h(t_s)(\Phi_l^h, \Phi_{rx}^u) \\
+ kA \sum_{i=M_1+1}^n \beta_i^u(t_s)(\nabla \Phi_i^u, \nabla \Phi_r^u) = k(f_1^s, \Phi_r^u) + \beta_r^u(t_{s-1}), \quad r = M_1 + 1, \dots, n, \\
\beta_r^v(t_s) + kf \sum_{i=M_1+1}^n \beta_i^u(t_s)(\Phi_i^u, \Phi_r^v) - kg' \sum_{l=M_2+1}^n \beta_l^h(t_s)(\Phi_l^h, \Phi_{ry}^v) \\
+ kA \sum_{j=M_1+1}^n \beta_j^v(t_s)(\nabla \Phi_j^v, \nabla \Phi_r^v) = k(f_2^s, \Phi_r^v) + \beta_r^v(t_{s-1}), \quad r = M_1 + 1, \dots, n, \\
\beta_\ell^h(t_s) + kH \sum_{l=M_2+1}^n \beta_l^h(t_s)(\Phi_l^h, \Phi_{\ell x}^u) + kH \sum_{l=M_2+1}^n \beta_l^h(t_s)(\Phi_l^h, \Phi_{\ell y}^v) = \beta_\ell^h(t_{s-1}), \\
\ell = M_2 + 1, \dots, n, s = 1, 2, \dots, n,
\end{array} \right. \quad (3.9)$$

along with the initial condition

$$\left\{ \begin{array}{l}
\beta_i^u(0) = (u(x, y, 0) - \bar{u}(x, y), \Phi_i^u(x, y)), \quad M_1 \leq i \leq n, \\
\beta_i^v(0) = (v(x, y, 0) - \bar{v}(x, y), \Phi_i^v(x, y)), \quad M_1 \leq i \leq n, \\
\beta_\ell^h(0) = (v(x, y, 0) - \bar{v}(x, y), \Phi_\ell^v(x, y)), \quad M_2 \leq \ell \leq n.
\end{array} \right. \quad (3.10)$$

Equations (3.9) can be written as in the following vector format

$$\begin{pmatrix} \beta_u^s \\ \beta_v^s \\ \beta_h^s \end{pmatrix} = k \begin{pmatrix} -AD_1 & fB & g'C_1 \\ -fB^T & -AD_2 & g'C_2 \\ -HC_1^T & -HC_2^T & \mathbf{O} \end{pmatrix} \begin{pmatrix} \beta_u^s \\ \beta_v^s \\ \beta_h^s \end{pmatrix} + k \begin{pmatrix} F_1^s \\ F_2^s \\ \mathbf{0} \end{pmatrix} + \begin{pmatrix} \beta_u^{s-1} \\ \beta_v^{s-1} \\ \beta_h^{s-1} \end{pmatrix}, \quad 1 \leq s \leq n, \quad (3.11)$$

where \mathbf{O} is a $(n - M_2) \times (n - M_2)$ zero matrix, and

$$\beta_u^s = (\beta_{M_1+1}^u(t_s), \dots, \beta_n^u(t_s))^T, \quad \beta_v^s = (\beta_{M_1+1}^v(t_s), \dots, \beta_n^v(t_s))^T,$$

$$\beta_h^s = (\beta_{M_2+1}^h(t_s), \dots, \beta_n^h(t_s))^T \quad (1 \leq s \leq n),$$

$$D_1 = \int_{\Omega} (\nabla \Phi_{M_1+1}^u, \dots, \nabla \Phi_n^u)^T (\nabla \Phi_{M_1+1}^u, \dots, \nabla \Phi_n^u) dx dy,$$

$$D_2 = \int_{\Omega} (\nabla \Phi_{M_1+1}^v, \dots, \nabla \Phi_n^v)^T (\nabla \Phi_{M_1+1}^v, \dots, \nabla \Phi_n^v) dx dy,$$

$$B = \int_{\Omega} (\Phi_{M_1+1}^v, \dots, \Phi_n^v)^T (\Phi_{M_1+1}^u, \dots, \Phi_n^u) dx dy,$$

$$C_1 = \int_{\Omega} (\Phi_{M_2+1}^h, \dots, \Phi_n^h)^T ((\Phi_{M_1+1}^u)_x, \dots, (\Phi_n^u)_x) dx dy,$$

$$C_2 = \int_{\Omega} (\Phi_{M_2+1}^h, \dots, \Phi_n^h)^T ((\Phi_{M_1+1}^v)_y, \dots, (\Phi_n^v)_y) dx dy,$$

$$F_1^s = ((f_1^s, \Phi_{M_1+1}^u), \dots, (f_1^s, \Phi_n^u))^T,$$

$$F_2^s = ((f_2^s, \Phi_{M_1+1}^v), \dots, (f_2^s, \Phi_n^v))^T.$$

Since it is well known (see [9]) that

$$\begin{aligned}
& \| (\Phi_1^u, \dots, \Phi_{M_1}^u, \Phi_{M_1+1}^u, \dots, \Phi_n^u, \Phi_1^v, \dots, \Phi_{M_1}^v, \Phi_{M_1+1}^v, \dots, \Phi_n^v; \Phi_1^h, \dots, \Phi_{M_2}^h, \Phi_{M_2+1}^h, \dots, \Phi_n^h) \\
& \quad - (\Phi_1^u, \dots, \Phi_{M_1}^u, 0, \dots, 0; \Phi_1^v, \dots, \Phi_{M_1}^v, 0, \dots, 0; \Phi_1^h, \dots, \Phi_{M_2}^h, 0, \dots, 0) \|_0^2 \\
& = \sum_{i=M_1+1}^n \lambda_i^u + \sum_{i=M_1+1}^n \lambda_i^v + \sum_{i=M_2+1}^n \lambda_i^h,
\end{aligned} \tag{3.12}$$

we obtain

$$\| (u_h^s - u_{M_1}^s), (v_h^s - v_{M_1}^s), (h_h^s - h_{M_2}^s) \|_0 \leq \| (\beta_u^s, \beta_v^s, \beta_h^s)^T \|_2 \sqrt{\sum_{i=M_1+1}^n \lambda_i^u + \sum_{i=M_1+1}^n \lambda_i^v + \sum_{i=M_2+1}^n \lambda_i^h}, \tag{3.13}$$

where $s = 1, 2, \dots, n$. From the inverse inequality (see [27] or [28]) and matrix normal property,

we obtain

$$\begin{aligned}
\| C_1 \|_2 & \leq \| (\Phi_{M_2+1}^h, \dots, \Phi_n^h)^T \|_0 \| (\Phi_{M_1+1}^u, \dots, \Phi_n^u)_x \|_0 \\
& \leq c\hbar^{-1} \| (\Phi_{M_2+1}^h, \dots, \Phi_n^h) \|_0 \| (\Phi_{M_1+1}^u, \dots, \Phi_n^u) \|_0 \leq c\hbar^{-1} \sqrt{\sum_{i=M_2+1}^n \lambda_i^h} \sqrt{\sum_{i=M_1+1}^n \lambda_i^u},
\end{aligned} \tag{3.14}$$

$$\begin{aligned}
\| C_2 \|_2 & \leq \| (\Phi_{M_2+1}^h, \dots, \Phi_n^h)^T \|_0 \| (\Phi_{M_1+1}^v, \dots, \Phi_n^v)_y \|_0 \\
& \leq c\hbar^{-1} \| (\Phi_{M_2+1}^h, \dots, \Phi_n^h) \|_0 \| (\Phi_{M_1+1}^v, \dots, \Phi_n^v) \|_0 \leq c\hbar^{-1} \sqrt{\sum_{i=M_2+1}^n \lambda_i^h} \sqrt{\sum_{i=M_1+1}^n \lambda_i^v},
\end{aligned} \tag{3.15}$$

$$\| B \|_2 \leq \| (\Phi_{M_1+1}^v, \dots, \Phi_n^v)^T \|_0 \| (\Phi_{M_1+1}^u, \dots, \Phi_n^u) \|_0 = \sqrt{\sum_{i=M_1+1}^n \lambda_i^v} \sqrt{\sum_{i=M_1+1}^n \lambda_i^u}, \tag{3.16}$$

$$\| F_1^s \|_2 \leq \| f_1^s \|_2 \| (\Phi_{M_1+1}^u, \dots, \Phi_n^u) \|_2 = \| f_1^s \|_2 \sqrt{\sum_{i=M_1+1}^n \lambda_i^u}, \tag{3.17}$$

$$\| F_2^s \|_2 \leq \| f_2^s \|_2 \| (\Phi_{M_1+1}^v, \dots, \Phi_n^v) \|_2 = \| f_2^s \|_2 \sqrt{\sum_{i=M_1+1}^n \lambda_i^v}. \tag{3.18}$$

Then, multiplying (3.11) by $((\beta_u^s)^T, (\beta_v^s)^T, (\beta_h^s)^T)$, one could get

$$\begin{pmatrix} \beta_u^s \\ \beta_v^s \\ \beta_h^s \end{pmatrix}^T \begin{pmatrix} \beta_u^s \\ \beta_v^s \\ \beta_h^s \end{pmatrix} = k \begin{pmatrix} \beta_u^s \\ \beta_v^s \\ \beta_h^s \end{pmatrix}^T \begin{pmatrix} -AD_1 & fB & g'C_1 \\ -fB^T & -AD_2 & g'C_2 \\ -HC_1^T & -HC_2^T & \mathbf{O} \end{pmatrix} \begin{pmatrix} \beta_u^s \\ \beta_v^s \\ \beta_h^s \end{pmatrix} + k \begin{pmatrix} \beta_u^s \\ \beta_v^s \\ \beta_h^s \end{pmatrix}^T \begin{pmatrix} F_1^s \\ F_2^s \\ 0 \end{pmatrix} + \begin{pmatrix} \beta_u^s \\ \beta_v^s \\ \beta_h^s \end{pmatrix}^T \begin{pmatrix} \beta_u^{s-1} \\ \beta_v^{s-1} \\ \beta_h^{s-1} \end{pmatrix}. \tag{3.19}$$

Noting that $A(\beta_u^s)^T D_1 \beta_u^s > 0$ and $A(\beta_v^s)^T D_2 \beta_v^s > 0$, if $\max\{\sqrt{\sum_{i=M_1+1}^n \lambda_i^u}, \sqrt{\sum_{i=M_1+1}^n \lambda_i^v}\} \leq \hbar/c$

(which is reasonable), by using matrix normal property, and (3.11), (3.14)~(3.19), one can obtain

$$\| (\beta_u^s, \beta_v^s, \beta_h^s)^T \|_2 \leq kc_0 \| (\beta_u^s, \beta_v^s, \beta_h^s)^T \|_2 + kC_0^s + \| (\beta_u^{s-1}, \beta_v^{s-1}, \beta_h^{s-1})^T \|_2, \tag{3.20}$$

where $c_0 = 2f \sqrt{\sum_{i=M_1+1}^n \lambda_i^u} \sqrt{\sum_{i=M_1+1}^n \lambda_i^v} + 2g' \sqrt{\sum_{i=M_2+1}^n \lambda_i^h} + 2H \sqrt{\sum_{i=M_2+1}^n \lambda_i^h}$, $C_0^s = \| f_1^s \|_2 \sqrt{\sum_{i=M_1+1}^n \lambda_i^u} + \| f_2^s \|_2 \sqrt{\sum_{i=M_1+1}^n \lambda_i^v}$.

Summing (3.20) from 1 to s , if k is sufficiently small such that $1 - c_0 k \leq 1/2$, yields

$$\|(\beta_u^s, \beta_v^s, \beta_h^s)^T\|_2 \leq k c_0 \sum_{i=0}^{s-1} \|(\beta_u^i, \beta_v^i, \beta_h^i)^T\|_2 + \bar{C}_1 \sqrt{\sum_{i=M_1+1}^n \lambda_i^u} + \bar{C}_2 \sqrt{\sum_{i=M_1+1}^n \lambda_i^v} + \|(\beta_u^0, \beta_v^0, \beta_h^0)^T\|_2, \quad (3.21)$$

where $(\beta_u^0, \beta_v^0, \beta_h^0)^T = (\beta_{M_1+1}^u(0), \dots, \beta_n^u(0), \beta_{M_1+1}^v(0), \dots, \beta_n^v(0), \beta_{M_2+1}^h(0), \dots, \beta_n^h(0))$, $\bar{C}_1 = 2k \sum_{i=1}^n \|f_1^s\|_2$, $\bar{C}_2 = 2k \sum_{i=1}^n \|f_2^s\|_2$. Noting that

$$\begin{aligned} \|(\beta_u^0, \beta_v^0, \beta_h^0)^T\|_2 &\leq (\|u(x, y, 0)\|_0 + \|\bar{u}\|_0) \|(\Phi_{M_1+1}^u, \dots, \Phi_n^u)\|_2 \\ &\quad + (\|v(x, y, 0)\|_0 + \|\bar{v}\|_0) \|(\Phi_{M_1+1}^v, \dots, \Phi_n^v)\|_2 \\ &\quad + (\|h(x, y, 0)\|_0 + \|\bar{h}\|_0) \|(\Phi_{M_2+1}^h, \dots, \Phi_n^h)\|_2 \\ &\leq \bar{C}_3 \left(\sqrt{\sum_{i=M_1+1}^n \lambda_i^u} + \sqrt{\sum_{i=M_1+1}^n \lambda_i^v} + \sqrt{\sum_{i=M_2+1}^n \lambda_i^h} \right), \end{aligned} \quad (3.22)$$

where $\bar{C}_3 = \max\{\|u(x, y, 0)\|_0 + \|\bar{u}\|_0, \|v(x, y, 0)\|_0 + \|\bar{v}\|_0, \|h(x, y, 0)\|_0 + \|\bar{h}\|_0\}$. Using discrete Gröwall inequality for (3.21), one could obtain

$$\|(\beta_u^s, \beta_v^s, \beta_h^s)^T\|_2 \leq \bar{C}_4 \left(\sqrt{\sum_{i=M_1+1}^n \lambda_i^u} + \sqrt{\sum_{i=M_1+1}^n \lambda_i^v} + \sqrt{\sum_{i=M_2+1}^n \lambda_i^h} \right), \quad (3.23)$$

where $\bar{C}_4 = \exp(nkc_0) \max\{\bar{C}_1 + \bar{C}_3, \bar{C}_2 + \bar{C}_3, \bar{C}_3\}$. Combining (3.13) with (3.23) and using Cauchy inequality yields the following result.

Theorem 1. *If $\max\{\sqrt{\sum_{i=M_1+1}^n \lambda_i^u}, \sqrt{\sum_{i=M_1+1}^n \lambda_i^v}\} \leq \hbar/c$ and k is sufficiently small, then*

the error estimate between the solutions for full basic Problem (II) and the solutions for the reduced order basic Problem (IV) is

$$\|(u_h^s - u_{M_1}^s), (v_h^s - v_{M_1}^s), (h_h^s - h_{M_2}^s)\|_0 \leq \bar{C}_5 \left(\sum_{i=M_1+1}^n \lambda_i^u + \sum_{i=M_1+1}^n \lambda_i^v + \sum_{i=M_2+1}^n \lambda_i^h \right), 1 \leq s \leq n, \bar{C}_5 = 3\bar{C}_4. \quad (3.24)$$

Combining (3.1) with (3.21) could yield in the following result.

Theorem 2. *If $\max\{\sqrt{\sum_{i=M_1+1}^n \lambda_i^u}, \sqrt{\sum_{i=M_1+1}^n \lambda_i^v}\} \leq \hbar/c$ and k is sufficiently small, then the*

error estimate between the solutions for Problem (II) and the solutions for the reduced order basic Problem (IV) is

$$\left\{ \begin{array}{l} \|u(t_s) - u_{M_1}^s\|_0 \leq c(\hbar^m + k) + \bar{C}_5 \left(\sum_{i=M_1+1}^n \lambda_i^u + \sum_{i=M_1+1}^n \lambda_i^v + \sum_{i=M_2+1}^n \lambda_i^h \right), \\ \|v(t_s) - v_{M_1}^s\|_0 \leq c(\hbar^m + k) + \bar{C}_5 \left(\sum_{i=M_1+1}^n \lambda_i^u + \sum_{i=M_1+1}^n \lambda_i^v + \sum_{i=M_2+1}^n \lambda_i^h \right), \\ \|h(t_s) - h_{M_2}^s\|_0 \leq c(\hbar^m + k) + \bar{C}_5 \left(\sum_{i=M_1+1}^n \lambda_i^u + \sum_{i=M_1+1}^n \lambda_i^v + \sum_{i=M_2+1}^n \lambda_i^h \right), \end{array} \right. \quad 1 \leq s \leq n. \quad (3.25)$$

Remark. In general, $c_0 = 2f \sqrt{\sum_{i=M_1+1}^n \lambda_i^u} \sqrt{\sum_{i=M_1+1}^n \lambda_i^v} + 2g \sqrt{\sum_{i=M_2+1}^n \lambda_i^h} + 2H \sqrt{\sum_{i=M_2+1}^n \lambda_i^h}$ is a very

small value so that $\exp(kc_0s)$ ($1 \leq s \leq n$) approaches 1, and taking $m = 1$ or 2 is sufficient in actual numerical simulation. In this paper, our reduced order basis methods come from the full order numerical computations, therefore, our aim is to start from Problem (II), then to analyze the error of Problem (IV). However, actual numerical computation should directly solve Problem (IV) getting $(\beta_i^s, \beta_i^s, \beta_j^s)^T$ ($1 \leq s \leq n, 1 \leq i \leq M_1, 1 \leq j \leq M_2$) such that (3.24) is satisfied if the reduced order basis is obtained from system trajectories obtained via experiments, or analytical derivations. Since, in general, M_1 and $M_2 \ll n$, it is only necessary to solve Problem (IV) with very few freedom degrees. In next section, we employ some examples to validate Theorem 1 and Theorem 2.

4. Some numerical examples

In this section we present numerical computations related to the approaches presented in the previous paragraphs. We first solve Problem (II) and Problem (IV) taking parameters as displayed in Table 1, and taking $T_1 = 1$ years, Ω varying from 30° S to 30° N in latitude and from 130° E to 70° W in longitude, time step is $k = 1/n$, and we obtain the results which are depicted graphically in Figure 3 and Figure 5 when $n = 5, 20$, and 30 , respectively. In order to obtain the POD approximate solutions for an error of less than 0.0007 which is used with (3.24), it is necessary to take $M_1 = M_2 \geq 3$ if $n = 5$, $M_1 = M_2 \geq 7$ if $n = 20$, and $M_1 = M_2 \geq 9$ if $n = 30$. However, we have the results of numerical simulations which are also depicted from Figure 3 to Figure 4, where Figure 2 displays profiles of the error and Figure 3 to Figure 4 exhibit profiles of the upper layer water thickness, and current velocity taking $M_1 = M_2 = 3$ if $n = 5$, $M_1 = M_2 = 7$ if $n = 20$, and $M_1 = M_2 = 9$ if $n = 30$, respectively. These profiles demonstrate that the results of the numerical simulations coincide with

the theory and the actual cases. Especially, when $n = 30$, it is necessary to solve the POD reduced Problem (IV) with equation numbers 30% less than required by the full order Problem (II). Therefore, the POD reduced method is very suitable for dealing with large-scale science engineering computations, and could simplify computing and reduce both CPU and memory requirements in the actual computational process in a sense that guarantees a sufficiently accurate numerical solution.

Acknowledgement

The first and second authors acknowledge the support of the National Science Foundation of China number 10471100 and 40437017, and Beijing Jiaotong University Science Technology Foundation.

References

- [1] M. A. Cane, The response of an equatorial ocean to simple wind stress patterns: Part I. Model formulation and analytical results, *J. Mar. Res.* 37 (1979) 233–252.
- [2] R. Seager, S. E. Zebiak, M. A. Cane, A model of the tropical Pacific sea surface temperature climatology, *J. Geophys. Res.* 93 (1988) 1265–1280.
- [3] L. Yu, J. J. O'Brien, Variational data assimilation for determining the seasonal net surface flux using a tropical Pacific Ocean model, *Journal of Physical Oceanography*, 5(1995) 2319–2343.
- [4] K. Fukunaga, *Introduction to Statistical Recognition*, Academic Press, 1990.
- [5] I. T. Jolliffe, *Principal Component Analysis*, Springer-Verlag, 2002.
- [6] D.T. Crommelin, A.J. Majda, Strategies for model reduction: comparing different optimal bases, *J. Atmos. Sci.* 61(2004) 2206–2217.
- [7] A.J. Majda, I. Timofeyev, E. Vanden-Eijnden, Systematic strategies for stochastic mode reduction in climate, *J. Atmos. Sci.* 60 (2003) 1705–1722.
- [8] F. Selten, Baroclinic empirical orthogonal functions as basis functions in an atmospheric model, *J. Atmos. Sci.* 54 (1997) 2100–2114.
- [9] P. Holmes, J. L. Lumley, G. Berkooz, *Turbulence, Coherent Structures, Dynamical Systems and Symmetry*, Cambridge University Press, Cambridge, UK, 1996.
- [10] G. Berkooz, P. Holmes, J. L. Lumley, The proper orthogonal decomposition in analysis of turbulent flows. *Annual Review of Fluid Mechanics* 25 (1993) 539–575.
- [11] W. Cazemier, R. W. C. P. Verstappen, A. E. P. Veldman, Proper orthogonal decomposition and low-dimensional models for driven cavity flows, *Phys. Fluids* 10 (1998) 1685–1699.
- [12] D. Ahlman, F. Serlund, J. Jackson et al, Proper orthogonal decomposition for time dependent lid-driven cavity flows, Research Report of Science Technology at University of Florida, 2005.
- [13] J. L. Lumley, Coherent Structures in Turbulence, in Meyer R E (ed.), *Transition and Turbulence*, Academic Press, 1981: pp. 215–242.
- [14] N. Aubry, P. Holmes, J. L. Lumley et al, The dynamics of coherent structures in the wall region of a turbulent boundary layer, *Journal of Fluid Dynamics*, 192(1988) 115–173.
- [15] L. Sirovich, Turbulence and the dynamics of coherent structures: Part I-III, *Quarterly of Applied Mathematics*, 45(3) (1987) 561–590.
- [16] R. D. Roslin, M. D. Gunzburger, R. Nicolaidis, et al, A self-contained automated methodology for optimal

- flow control validated for transition delay, *AIAA Journal* 35 (1997) 816—824.
- [17] H.V. Ly, H. T. Tran, Proper Orthogonal Decomposition for Flow Calculations and Optimal Control in a Horizontal CVD Reactor, Technical Report, CRSC-TR98-12 (Center for Research in Scientific Computation), North Carolina State University, 1998.
- [18] J. Ko, A. J. Kurdila, O. K. Redonitis et al, Synthetic Jets, Their Reduced Order Modeling and Applications to Flow Control, AIAA Paper number 99-1000, 37th Aerospace Sciences Meeting & Exhibit, Reno, 1999.
- [19] P. Moin, R D. Moser, Characteristic-eddy decomposition of turbulence in channel, *Journal of Fluid Mechanics* 200 (1989) 417—509.
- [20] M .Rajaei, S. K F. Karlsson, L. Sirovich, Low dimensional description of free shear flow coherent structures and their dynamical behavior. *Journal of Fluid Mechanics*, 258(1994) 1401—1402.
- [21] Y. H. Cao, J. Zhu, Z. D. Luo, I. M. Navon, Reduced order modeling of the upper tropical Pacific ocean model using proper orthogonal decomposition, *Computers & Mathematics with Applications* 2005. In press.
- [22] H.V. Ly, H.T. Tran, Proper orthogonal decomposition for flow calculations and optimal control in a horizontal CVD reactor. *Quarterly of Applied Mathematics* 60(4) (2002) 631—656,.
- [23] L. Sirovich, Turbulence and the dynamics of coherent structures, parts I-III, *Q. Appl. Math.* XLV (3)(1987) 561—590.
- [24] R A. Adams, *Sobolev Space*. New York: Academic Press, 1975.
- [25] Z. D., Luo , J. Zhu, Q .C. ,Zen et al, Mixed finite element methods for the shallow water equations including current and silt sedimentation (I), the continuous-time case, *Applied Mathematics and Mechanics*, 25(1) (2004) 80—92.
- [26] Z. D. Luo, J .Zhu, Q C .Zen, et al, Mixed finite element methods for the shallow water equations including current and silt sedimentation (II), the discrete-time case along characteristics, *Applied Mathematics and Mechanics*, 25(2) (2004) 186—202.
- [27] P. C. Ciarlet, *Finite Element Method for Elliptic Problems*, North—Holland, Amsterdam, 1978.
- [28] Z. D. Luo, *Mixed Finite Element Methods and Applications*, Beijing, Chinese Science Press, 2006.

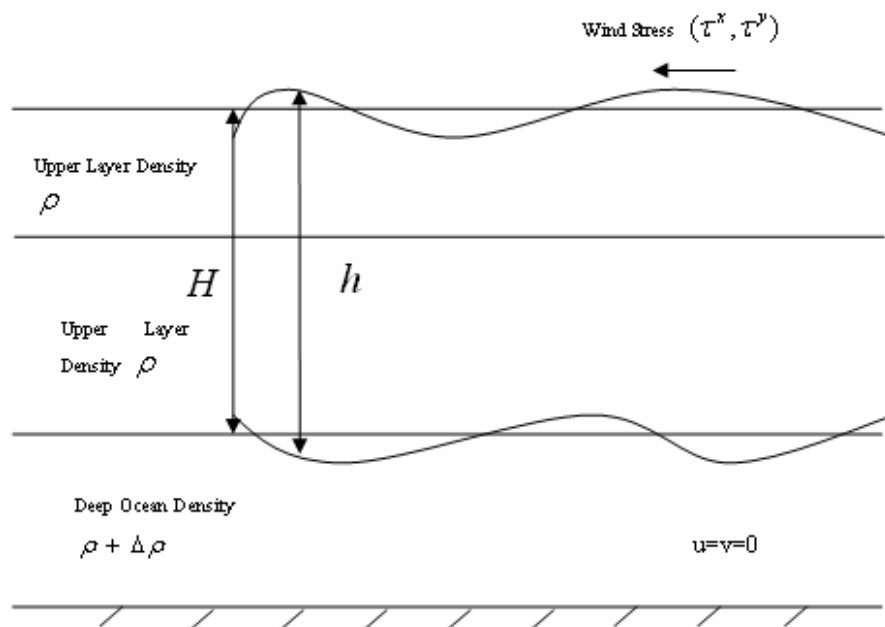


Fig. 1

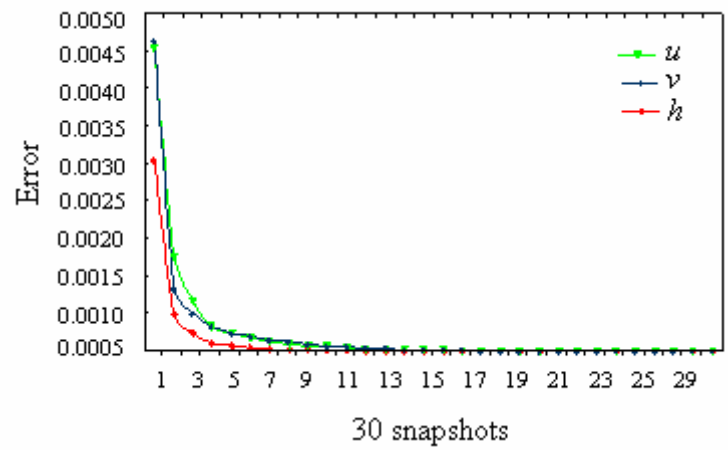
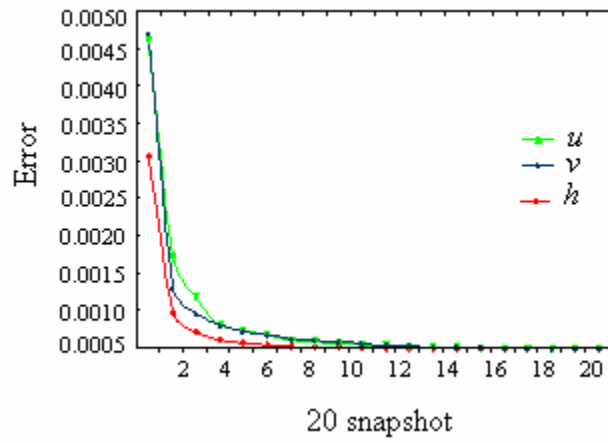
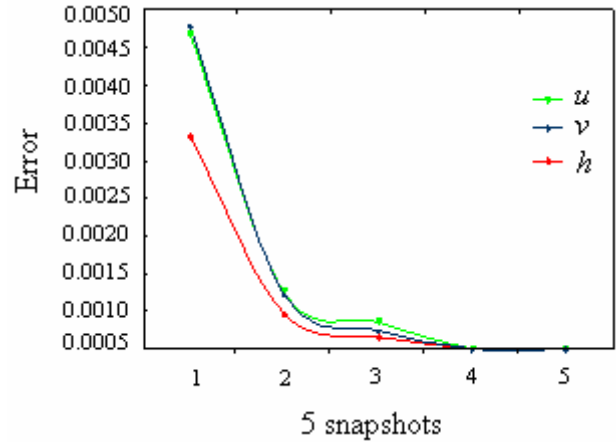
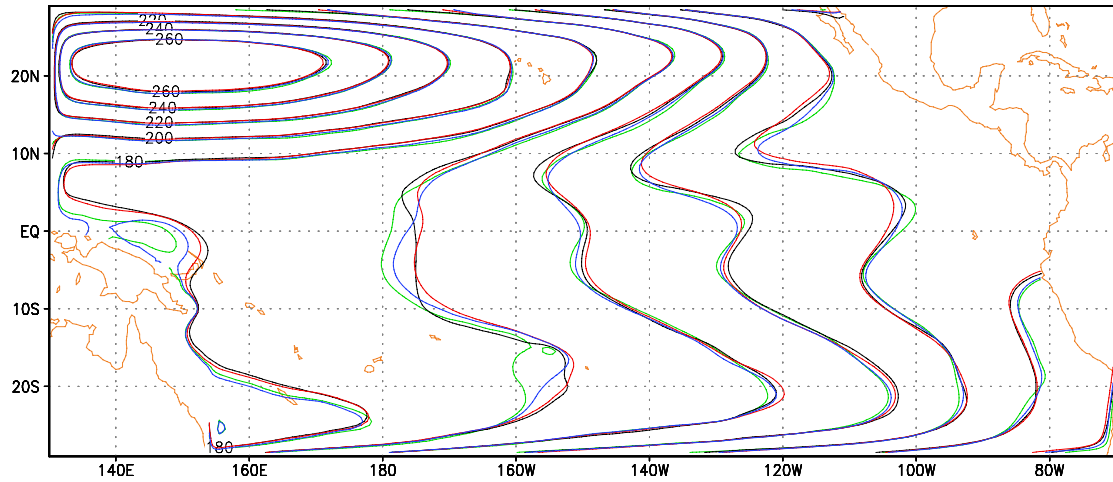
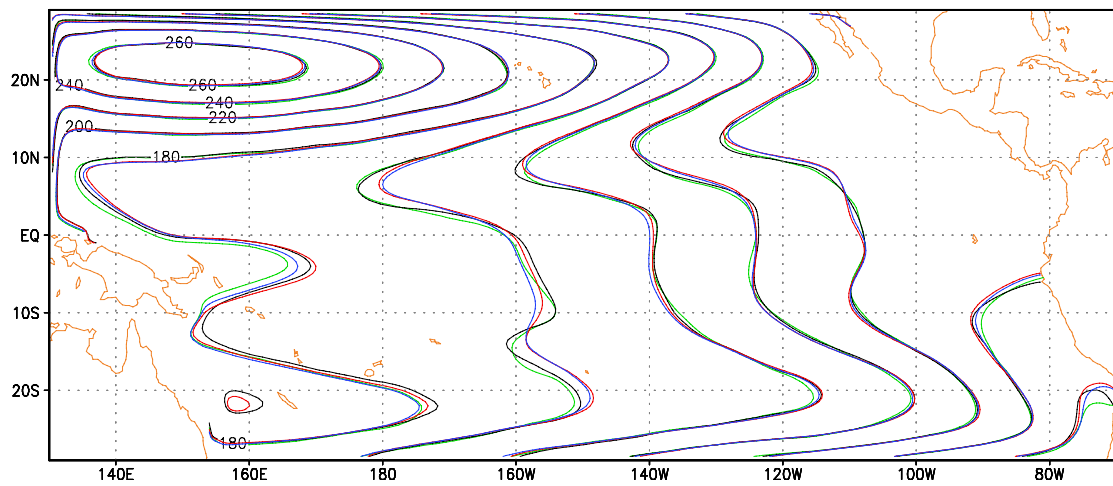


Fig2. Error profiles of $n = 5, 20,$ and 30

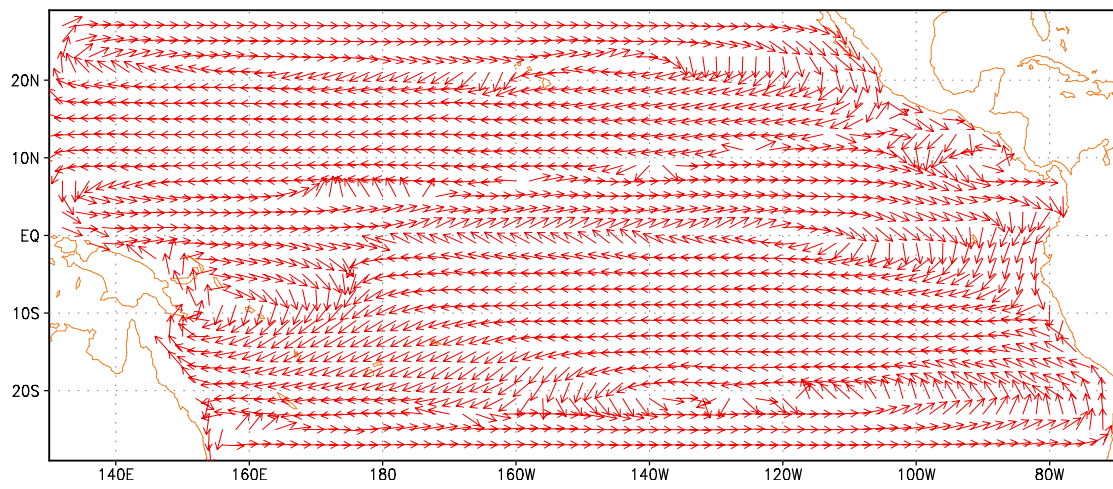
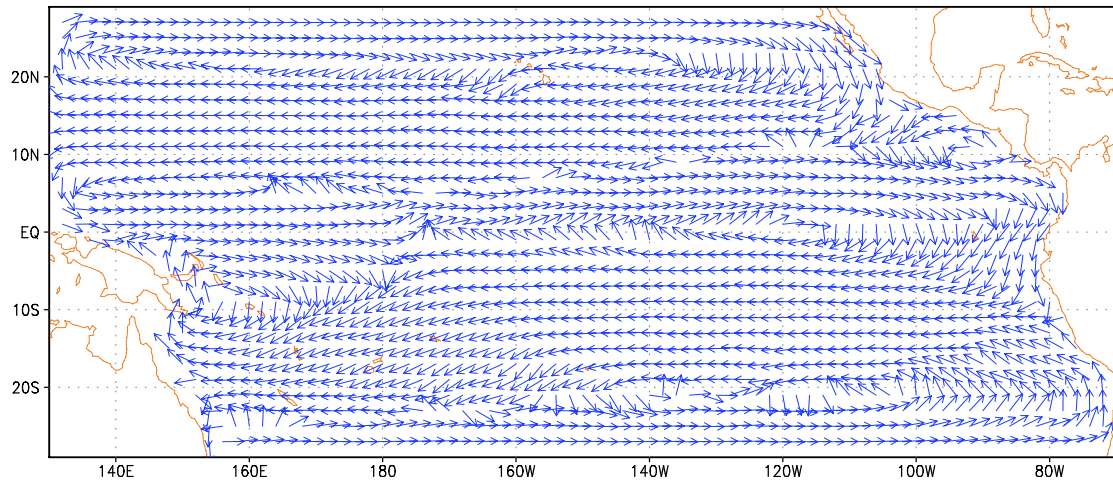


(a) June

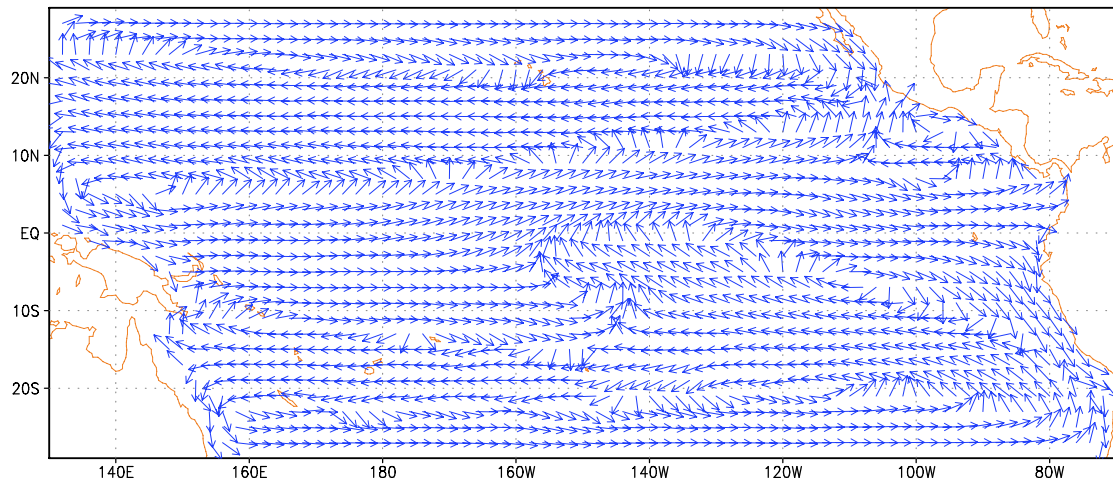


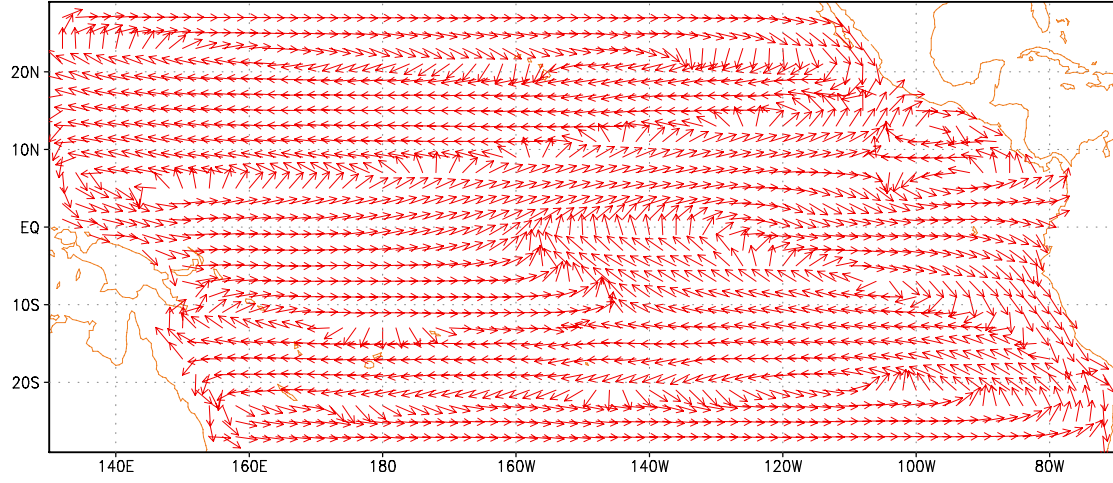
(b) December

Fig 3. Upper layer thickness in June and December in case of 5 snapshots, 20 snapshots, 30 snapshots, the full model approximation and the reduced order approximation. The dark: full order approximation, the green: 5 snapshots, the red: 20 snapshots, the purple: 30 snapshots.



(a) June





(b) December

Fig 4. Profiles of currents in June and December with 20 snapshots. The blue vector: full order approximation; the red vector: reduced order approximation.

| Parameter | Value | Remarks |
|-----------|------------------------------------|-------------------------------------|
| g' | 3.7×10^{-2} | Reduced gravity |
| C_D | 1.5×10^{-3} | Wind stress drag coefficient |
| H | 150 m | Mean depth of upper layer |
| ρ_a | 1.2 kg m^{-3} | Density of air |
| ρ_0 | 1025 kg m^{-3} | Density of seawater |
| A | $750 \text{ m}^2 \text{ sec}^{-1}$ | Coefficient of horizontal viscosity |

Table 1. parameters of Problem (II) and Problem (IV)